FAINT STELLAR PHOTOMETRY IN CLUSTERS. II. NGC 6791 AND NGC 6535

BARBARA J. ANTHONY-TWAROG[1] AND BRUCE A. TWAROG
Department of Physics and Astronomy, University of Kansas at Lawrence

ABSTRACT

Video Camera photometry of the clusters NGC 6791 and NGC 6535 obtained with the Kitt Peak National Observatory 2.1 m telescope is presented.

For the open cluster NGC 6791, the new data provide improved delineation of the cluster color-magnitude diagram in the region of the turnoff and fainter, revealing a morphology very similar to that of NGC 188. Assuming that NGC 6791 and NGC 188 have the same metallicity and adopting $E(B-V) = 0.20$, NGC 6791 is found to be intermediate in age between NGC 188 and Melotte 66. The apparent distance modulus of NGC 6791 is 2.2 mag larger than that of NGC 188; this is equivalent to $(m - M) = 13.5$ using the $Y = 0.3$ Yale isochrones and $(m - M) = 13.2$ using the $Y = 0.2$ isochrones of VandenBerg. Independent of the choice of models, it appears that the red-giant clump in both clusters may provide support for a strong metallicity and age effect on the absolute magnitude of the horizontal branch.

For the sparse globular NGC 6535, the photometry reveals a color-magnitude diagram essentially identical to that of M13, with an age comparable to that found for other globulars. No evidence is found for a significant population of blue stragglers in the cluster core.

Details of a calibrated technique for deriving the age of an old cluster using color-magnitude–diagram morphology, independent of reddening and only weakly dependent in metallicity, are presented in an appendix.

Subject headings: clusters: globular — clusters: open — photometry — stars: evolution

I. INTRODUCTION

Studies of galactic structure, chemical evolution, and stellar populations in our own and other galaxies have progressed in great measure due to studies in open and globular clusters. Initial concerns with determination of cluster distances and ages have expanded, in recent years, to explore more fully the observable differences in color-magnitude (cm)–diagram morphology due to location in the Galaxy, age, helium abundance, and metallicity.

With the aim of reconstructing the earliest history of the disk and halo, and testing stellar evolution theory, the oldest disk clusters and the more accessible globulars have been studied extensively, but progress has been hampered by the very small number of ancient (age greater than 3×10^9 yr) open clusters, extreme distances and severe field crowding making photometric surveys frustratingly difficult. Unlike the globulars, for which horizontal branches provide a readily observed distance calibrator, photometry of main sequence stars at apparent magnitudes of 18–21 is necessary to determine distances for many open clusters.

The advent of higher quantum-efficiency linear area detectors and digital photometry algorithms has permitted broad extensions to cluster photometric studies by providing higher accuracy at fainter magnitudes and in considerably less observing time than for photographic plates. In a previous study, Frogel and Twarog (1983) employed the Vidicon area photometer at Cerro Tololo Inter-American Observatory to study the old open cluster NGC 2204 and the globular cluster E3, a relatively unusual application of this device. This paper will present the results of a *BV* photometric study of two northern

clusters, NGC 6791 and NGC 6535, using the Video Camera on the 2.1 m telescope at KPNO.

NGC 6791 has long been known to be among the oldest open clusters in the Galaxy. This rich object was the subject to a classic photometric survey by Kinman (1965, hereafter KI) but has attracted little attention since then. The cm diagram of KI exhibits an extensive red-giant branch and well-defined red-giant clump. However, the main-sequence turnoff resembled that of a globular cluster in shape, but an open cluster in luminosity. Below the turnoff, increased photometric scatter made delineation of the main sequence difficult. Subsequent study by Harris and Canterna (1981) using classical photoelectric techniques revealed a systematic radial photometric error in the data of KI, making NGC 6791 a prime candidate for a larger scale photometric investigation.

NGC 6535 is a sparsely populated globular cluster which has had only one photometric study of the region near the giant branch (Liller 1980, hereafter LI). The low concentration of stars near the cluster core led to its selection as a test of the possibility that blue stragglers in globulars might be concentrated in the cluster nucleus, where observations are normally impossible.

The organization of the paper is as follows: § II details the acquisition and processing of the Video Camera (vc) photometry, § III and § IV discuss the results for NGC 6791 and NGC 6535 respectively, and § V provides a summary of the conclusions and plans for future research.

II. ACQUISITION AND INITIAL PROCESSING

All the photometric frames to be analyzed were obtained in 1981 September with the KPNO Video Camera on the 2.1 m telescope. The Video Camera is described in detail in Kitt Peak's observing manual for the instrument, but for a brief description, the camera may be thought of as composed of two stages: the first stage of the RCA 4849 ISIT tube employs an

image tube, which has approximately the response of an S-25 photocathode, coupled to a silicon-target vidicon which composes the second stage. The tube is read out every 1.6 s in a 256 × 256 pixel format. Since the field of view at the 2.1 m Cassegrain focus is approximately 110″ square, each pixel is about 0″.4 across.

A typical observing mode is to integrate for 512 readout cycles (13^{m}6) through the appropriate filters, although shorter integrations can be subsequently co-added to produce higher signal-to-noise pictures. The B "filter" is a combination of 2 mm quartz, 2 mm GG-385, 1 mm BG-18, and 1 mm BG-37 glasses to produce a bandpass of half-width 1125 Å centered on 4400 Å. The V "filter" is composed of 3 mm quartz, 1 mm BG-18, and 2 mm BG-495 to produce a bandpass of half-width 1171 Å centered on 5425 Å.

The Video Camera flat-field response for each filter must be measured by observing a diffused projector lamp and, if possible, the twilight sky and blank sky frames during each night. Full 13^{m}6 dark frames are obtained daily for the removal of bias. The initial processing of the frames entails co-adding similar frames, the subtraction of the dark frames, and the division by the flat-field response for each filter; these are carried out in a batch mode on the KPNO Cyber in Tucson. An additional step in the batch processing may be to remove the geometric distortion of the frames, which is consistent and well known. [If not removed prior to photometric reduction of the frames, a correction may be applied to each derived magnitude which is a function of the radial distance from the geometric center of the Video Camera array, pixel (x, y) = (150, 134).]

A preselected field which includes nearly all of the southwest quadrant from KI's photographic study in NGC 6791 was observed on 1981 September 3 and 5; neither night was entirely photometric. For the September 3 frames, two 6^{m}8 blue frames were co-added to be compared with one 13^{m}6 V frame. The September 5 observations combined for each of the two filters a 6^{m}8 and a 13^{m}6 observation.

The field selected for study in NGC 6535 on September 2 includes a fair portion of the center of this loose globular, as well as a number of stars to the southeast of the center which were included in LI's photometric survey. One B and two V frames were obtained September 2, each 13^{m}6 long. The observations of September 5 were displaced about 25″ to the southeast to avoid the very dense and bright concentration of stars near the center. Again, conditions were not consistently photometric; the seeing and transparency were conspicuously worse on the latter night, and the data have been used only to supplement the September 2 observations. The observations for September 5 consisted of four B and three V frames, each 6^{m}8 long.

III. NGC 6791

a) Reduction and Calibration of Data

We have selected a field in NGC 6791 with one corner positioned near the optical center of the cluster. The field, illustrated in Figure 1, which is a reproduction from Figure 2 of KI, incorporates the southwest quadrant of the two inner rings in KI's photographic survey. Crowding was not a severe problem, and fairly simple alogrithms were sufficient to derive magnitudes from the picture arrays.

The Kitt Peak Mountain Photometry Code (MPC) was used in 1983 May to process the NGC 6791 frames which were not previously corrected for geometric distortion. The MPC gener-

ates magnitude indices from comparison of intensity in the stellar image (within a specified pixel radius of the centroid of the image) and in a sky annulus around the star. Output for each preselected star image includes the derived instrumental magnitudes, an additive correction to the magnitude to remove the effect of geometric distortion, and two magnitude error estimates, one based on noise in the sky pixels, one based on noise in the object pixels; these are lower estimates only to the true instrumental magnitude error.

Ideally, one would transfer these instrumental magnitudes to the standard system using a set of photoelectric standards within each field, covering a wide range in $B-V$ to allow for color terms in the transformation. The sample of 143 stars measured includes a number of inner-ring southwest-quadrant stars from KI's photographic survey, as well as several in the second ring; two of the stars in ring two were measured photoelectrically by Harris and Canterna (1981), stars 31 and 35, but were too bright to be measurable in the videocamera frames.

Fortunately, the lack of standards is not an insurmountable problem, as the response of the Video Camera has been well-studied. Da Costa, Mould, and Ortolani (1984) have employed a calibration for the Kitt Peak 4 m Cassegrain Video Camera system of the form:

$$V = y + k_1$$
$$B-V = 1.5(b - y) + k_2$$

where y and b are the instrumental magnitudes, with k_1 and k_2 as zero-point corrections applied to the magnitudes and colors in each frame.

Given the slopes of the transformation, the zero points can be derived using the photographic data of KI for stars in the inner two rings. This would appear to be a hazardous approach in the case of NGC 6791, where the photoelectric standards with which KI calibrated his photographic photometry are at a considerable distance from the central area of the cluster.

Whether the cause is a nonuniform plate background over the range from the photoelectric standard area to the central region of the cluster, or merely the increased stellar background in the center of the cluster, there is evidence for a radial systematic error in KI's photographic photometry. Harris and Canterna (1981) compared stars in rings one and two of KI's survey with photoelectric BV measurements, finding that the photographic values for the innermost ring stars are too bright by 0.02 mag and too blue, by 0.07 mag, compared to the photoelectric values, and the ring two stars too red by 0.05 mag.

With these estimates of the systematic errors in the photographic magnitudes and colors, it has been possible to "correct" KI's measurements for stars in our field in order to minimize the radial systematic error. Table 1 lists the stars used to calibrate the frames in NGC 6791. The values for V and $(B-V)$ are the values from KI's photographic study, corrected by the amounts suggested by Harris and Canterna. When these values are compared to the instrumental magnitudes according to the linear form of calibration noted above, an internal dispersion of 0.05 in V and 0.08 in $(B-V)$ is obtained. Identical dispersions are obtained if stars from rings one and two are considered separately, lending confidence to the corrections suggested by Harris and Canterna (1981). These values are also comparable to the formal instrumental magnitude errors derived in the MPC, which range from 0.01–0.04 at $V = 20$, and color errors of 0.02 to 0.09 for the faintest stars. These

FIG. 1.—Identification chart for stars in NGC 6791. All numbers in Ring 1 and those underlined in Ring 2 are on the system of KI. North is up, east is to the left. All others are program stars numbered for the current investigation. Chart is reproduced courtesy of T. D. Kinman and *The Astrophysical Journal*, published by the University of Chicago Press; © 1965 the American Astronomical Society.

TABLE 1

CALIBRATION SEQUENCE FOR NGC 6791

Star	V	$B-V$
SW Ring 1–21	16.53	0.82
SW Ring 1–25	17.38	0.96
SW Ring 1–26	18.26	0.83
SW Ring 1–29	18.39	0.89
SW Ring 1–38	19.37	0.81
SW Ring 1–39	18.72	0.88
SW Ring 1–40	18.74	0.89
SW Ring 1–43	17.47	0.95
SW Ring 1–48	17.91	0.82
Ring 2–33	16.60	1.23
Ring 2–34	16.83	1.15
Ring 2–39	16.97	0.89

estimates indicate the random internal error per star; the possible systematic departures from the standard BV system are estimated to be 0.05 in V and 0.04 in $(B-V)$, based on the errors associated with Harris and Canterna's photoelectric corrections, plus the estimated error in the intercept of each linear calibration fit.

The calibrated photometry for stars in NGC 6791 is listed in Table 2, where a note indicates whether single measures from 1981 September 3 or September 5 were used to yield the magnitude and color. A color-magnitude diagram of these points is shown in Figure 2.

Comparison of Figure 2 with Figure 3 of KI clearly shows a distinct difference in the region of the turnoff with the data of KI exhibiting a sharp turn toward the red above $V = 18$. The reality of this feature is crucial because the cm–diagram mor-

phology can be used to infer both an age and a metallicity when more direct measures are unavailable. As will be discussed below, the newer results are in excellent agreement with the cm–diagram morphology of the other well-studied cluster of comparable age, NGC 188, and imply that there is a significant error in the photometry of KI near the turnoff. There is weak evidence for the existence of a main-sequence gap at $V = 17.8$, comparable to that found in NGC 188 (McClure and Twarog 1977). However, analysis of this feature should await additional confirmation through astrometric and further photometric studies.

The photometry of Table 2 can be used to test two of the more uncertain aspects of the data-reduction procedure, the correction for geometric distortion and the zero point of the color calibration. cm-diagrams were constructed using stars near the geometric center of the Video Camera frames and stars in an outer annulus of the frames. Within the photometric uncertainties, the main-sequence ridge lines for the two samples showed no significant differences.

As a second test, using stars in ring two and beyond, a main-sequence ridge line was constructed. For the eight stars of ring one (one blue straggler was excluded from the analysis), the mean deviation of the stars from the ridge line in $(B-V)$ was determined to be less than 0.02 ± 0.04 mag in the sense (ring one − ring two). Had the color corrections of Harris and Canterna (1981) not been applied, an easily detected systematic color difference of -0.10 mag would be the result.

The small number of program stars in ring one also emphasizes the insensitivity of the color of the turnoff to the existence of the radial color gradient in the photometry of KI. The vc data for NGC 6791 should be on the same system as the photo-

TABLE 2

VIDEO CAMERA PHOTOMETRY IN NGC 6791

No.	V	$B-V$	Kinman Identification	No.	V	$B-V$	Kinman Identification
1......	17.64	0.86		31......	19.03	0.97	
2......	18.20	0.86		32......	18.28	0.94	
3......	18.32	0.83		33......	17.40	0.90	
4......	17.34	0.94		34......	18.60	0.94	
5......	18.62	0.89		35......	18.60	0.88	
6......	18.40	0.89		36......	18.50	0.00	
7......	19.02	1.01		37......	19.02	1.03	
8......	19.68	1.14		38......	18.20	0.92	
9......	18.86	0.83		39......	18.10	0.77	
10......	18.48	0.89		40......	19.22	1.02	
11......	17.34	1.13		41......	18.12	0.70	
12......	17.44	0.98		42......	17.78	0.83	
13......	17.52	0.81		43......	18.74	0.96	
14......	18.10	0.82		44......	18.05	0.85	
15......	17.38	0.81		45......	17.46	1.06	
16......	17.56	0.86		46......	17.98	0.94	
17......	17.56	0.82		47......	18.56	0.68	
18......	17.23	0.72		48......	17.02	0.90	Ring 2–39
19......	19.16	1.05		49......	19.19	1.00	
20......	19.09	0.94		50......	18.20	0.99	
21......	19.14	1.03		51......	18.11	0.86	
22......	17.97	0.86		52......	18.06	0.88	
23......	17.70	0.84		53......	17.39	0.84	
24......	18.32	0.80		54......	...	...	
25......	17.41	0.84		55......	18.51	0.83	
26......	19.52	1.01		56......	17.48	0.86	
27......	19.11	0.92		57......	17.63	0.81	
28......	18.62	0.58		58......	16.62	1.16	Ring 2–33
29......	18.70	0.94		59......	16.86	1.07	Ring 2–34
30......	20.20	1.64		60......	19.31	1.06	

TABLE 2—*Continued*

No.	V	B−V	Kinman Identification	No.	V	B−V	Kinman Identification
61	18.34	0.82		104	17.94	0.88	
62	18.81	0.91		105	18.32	0.92	
63	19.58	1.00		106	18.26	0.83	
64	17.45	0.82		107	17.83	0.85	
65	20.30	0.80		108	18.16	0.70	
66	17.56	0.83		109	18.25	0.85	
67	17.31	0.86		110	17.30	0.90	
68	17.78	0.77					
69	18.07	0.90		111	18.05	1.93	
70	19.45	1.08		112	18.04	0.92	
				113	18.64	0.98	
71	16.97	1.01		114[a]	18.04	0.84	
72	19.57	1.26		115[a]	18.46	0.90	
73	19.76	0.89		116	17.53	0.83	
74[a]	17.93	0.87		117	17.78	0.83	
75[a]	19.15	1.00		118	17.68	0.85	
76	17.54	0.85		119	19.17	1.07	
77	...	...		120	19.47	1.06	
78	17.55	0.73					
79	19.10	1.08		121	18.36	0.92	
80	19.33	0.99		122	18.24	0.86	
				123	17.51	0.80	
81	18.64	1.10		124	17.29	1.06	
82	18.08	0.89		125	...	...	
83	18.56	0.94		126	17.62	0.91	
84	19.38	0.98		127[a]	17.98	0.82	
85	...	...		128	17.48	0.83	SW Ring 1–43
86	18.98	0.93		129	18.64	0.97	SW Ring 1–39
87	18.56	0.95		130	18.72	0.92	SW Ring 1–40
88[a]	19.17	0.94					
89	19.76	1.20		131	17.94	0.86	SW Ring 1–48
90	17.38	0.88		132	19.39	0.91	SW Ring 1–38
				133	18.22	0.88	SW Ring 1–26
91	17.98	0.83		134	17.34	0.88	SW Ring 1–25
92	17.62	0.88		135[a]	16.61	0.72	SW Ring 1–21
93	18.24	0.85		136[a]	18.47	0.86	SW Ring 1–29
94	18.96	0.97		137	19.33	1.06	
95	19.30	1.06		138[a]	19.81	0.96	
96	17.56	0.84		139[a]	19.08	1.05	
97	18.24	0.89		140[a]	19.74	0.74	
98	17.68	1.02					
99	17.70	0.80		141	18.54	0.94	
100	19.16	0.90		142[a]	18.73	1.00	
				143[b]	17.54	0.84	
101	19.84	1.10		144[b]	20.23	0.87	
102	17.96	0.82		145[b]	18.92	0.93	
103	18.54	1.00		146[b]	18.78	0.86	

[a] One measurement only, on September 5.
[b] One measurement only, on September 3.

electric (pe) data of Harris and Canterna (1981). The corroboration of the need for a color correction to the data of KI as demonstrated above gives us confidence that the systematic error in the color zero point is probably less than the 0.05 mag color difference between the data of KI and that of Harris and Canterna (1981).

b) Reddening and Metallicity

KI derived a mean reddening of $E(B-V) = 0.22$ mag from MK classifications and $(B-V)$ colors of 16 probable members of NGC 6791. Given the photographic nature of the colors, Harris and Canterna (1981) attempted an improved estimate using UBV pe data and MK classifications for ten stars to derive $E(B-V) = 0.13 \pm 0.03$, considerably smaller than the value used by KI. However, this result must be regarded as uncertain for three reasons:

1. Two stars with the largest reddenings were dropped from the average for being more than 3 σ above the mean. Though nonmembers, both are foreground stars and should provide a lower limit to the reddening estimate. At least two of the stars included in the final average were nonmembers. Use of all 12 stars implies $E(B-V) = 0.16 \pm 0.02$.

2. Of the eight possible cluster members, five appear to be blue stragglers or evolved blue stragglers, i.e., they lie above the cluster turnoff and are bluer than the giant branch. This would imply that they have undergone anomalous evolution and may not be subject to the same color-spectral–type relation as "normal" stars.

3. There is a conspicuous difficulty in using spectral classification to determine unreddened colors for K giants; the differences in $(U-B)$ between adjacent K giant subclasses may be as large as 0.20 in the K2–K5 range.

We have chosen to employ Harris and Canterna's photoelectric colors for three K giants which were judged most likely to be members, stars 2001, 2008, and 2038, which are stars 1, 8, and 38 in ring two of KI's photographic survey. From Craw-
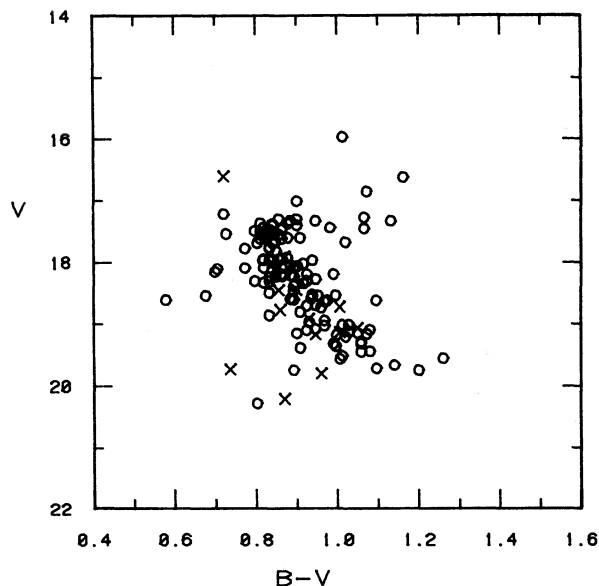
FIG. 2.—Color-magnitude diagram of Video Camera photometry in NGC 6791 as listed in Table 2. Open circles are observations averaged over two nights, crosses are single observations.

ford and Mandwewala's (1977) study of the relation between $(U-B)$ and $(B-V)$ color excesses, a reddening slope of 1.095 is found to be appropriate for mid-K giants. Tracing these stars back to the $(U-B)_0$, $(B-V)_0$ sequence for giants of FitzGerald (1970), a mean reddening of 0.20 ± 0.03 is derived. (Note that we are implicitly assuming that the metallicity of NGC 6791 is comparable to that of the nearby field stars.)

An additional comparison can be made to the reddening maps derived from neutral-hydrogen column-density and galaxy counts by Burstein and Heiles (1982). For the position of NGC 6791 at $(l, b) = (70°, 11°)$, a reddening of $E(B-V) = 0.17 \pm 0.02$ is indicated. $E(B-V) = 0.20$ will be adopted.

Until recently, the largest uncertainty in the discussion of this cluster was the metallicity; no reliable, direct measurement of the metal abundance had ever been made. KI used low-dispersion spectra and the width of the subgiant branch to infer a very approximate solar metallicity. Harris and Canterna (1981) used UBV photometry to derive an internally consistent $[Fe/H] = -0.2 \pm 0.3$ relative to the Sun. (Spinrad and Taylor 1971 have derived $[M/H] = +0.75$ from scanner data, but the problems associated with this technique have been well documented in the literature and will not be discussed further.)

We are thus faced with adopting a cluster metallicity based solely upon indirect techniques. The best approach available is similar to that adopted by KI, cm–diagram morphology in the region of the subgiant branch. Analysis of theoretical iso-chrones (e.g. Ciardullo and Demarque 1979) demonstrates that for clusters of a given age, metallicity changes the slope of the subgiant branch. As the metallicity increases, the subgiant branch at the level of the turnoff becomes increasingly horizontal, actually turning down toward fainter magnitudes as $(B-V)$ increases, for abundances near solar.

As will be demonstrated below, NGC 6791 appears to be only slightly older than NGC 188. A direct comparison of these two clusters is shown in Figure 3 where $E(B-V) = 0.08$ and $E(B-V) = 0.20$ have been adopted for NGC 188 and NGC 6791 respectively. The solid line is based on the normal points of NGC 188 from Twarog (1978, hereafter TW), shifted to

match the main sequence of NGC 6791. The improved delin-eation of the turnoff region from the vc data emphasizes the strong similarity of the two clusters and the likelihood that NGC 6791 is very similar in metallicity to NGC 188, i.e., solar metallicity. This indirect determination has now been corrobo-rated by direct photometric measurement. Geisler (private communication, 1984) using the Washington system and Janes (1984) using DDO photometry have derived solar metallicity for the cluster. Janes (1984) finds $[Fe/H] = -0.08 \pm 0.07$, adopting a significantly lower reddening of $E(B-V) = 0.10$. However, an increased reddening estimate will raise the metal-licity, not lower it, so the adopted reddening is not a problem.

c) Distance and Age

Given the reddening and metallicity, it should be possible to derive a reliable distance modulus through main-sequence fitting to other clusters of known distance or theoretical iso-chrones or both, and the cluster age by comparison with theo-retical models. As a first attempt we show the comparison between NGC 188 and NGC 6791 in Figure 3. Because they supposedly have the same metallicity, the only adjustment necessary is a correction for the difference in reddening and distance between the clusters. The apparent modulus of NGC 188 is 11.4 (TW) based on a comparison with the Hyades main sequence with appropriate metallicity corrections (Eggen and Sandage 1969), an increase in the Hyades distance modulus from 3.0 to approximately 3.3 (Hanson 1975), and an assumed reddening of $E(B-V) = 0.08$. Internal consistency among the main-sequence fits of NGC 188, NGC 6791, and the isochrones of Ciardullo and Demarque (1977) requires that the apparent modulus be lowered to $(m-M) = 11.3$. The normal points for NGC 188 in Figure 3 required an increase of 2.2 mag in V to match the cm–diagram of NGC 6791, implying an apparent modulus for the cluster of $(m-M) = 13.5$, or a true distance modulus of approximately 12.8.

An indirect check on this result can be made using the giant branch of the cluster, specifically the red-giant clump, the
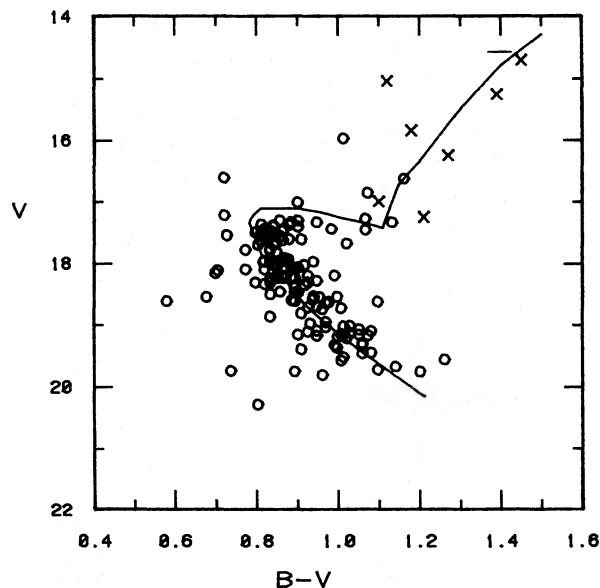

FIG. 3.—Comparison of data in Table 2 with the normal point sequence for NGC 188 reddened by $E(B-V) = 0.20$ and shifted in apparent distance modulus by 2.2 mag. Crosses are photoelectric data for giants from Harris and Canterna 1981.

open-cluster analog of the horizontal branch. In addition to the photometric results of the present study, some of the pe data of Harris and Canterna (1981) have been plotted in Figure 3 to identify the location of the giant branch of NGC 6791, and the location of the red-giant clump in NGC 188 is indicated.

The luminosity of the clump stars is a function of the core mass and the helium abundance, with the higher core-mass and higher helium-abundance stars being brighter. Increased metallicity should lead to a fainter clump luminosity (Iben 1974), though the size of the effect is a matter of dispute (Sandage 1982). The work of Cannon (1970) indicates that in open clusters older than 1×10^9 yr, the absolute magnitude of the clump is effectively constant.

Of the well-defined calibration clusters discussed in the Appendix, main-sequence fits to the Hyades with appropriate metallicity corrections are available for two, NGC 752 and M67. There is also $uvby$ Hβ photometry available for NGC 752. The distance moduli for these clusters, $(m-M)_0 = 9.7$ for M67 and $(m-M)_0 = 8.2$ for NGC 752, lead to clump absolute magnitudes of 0.7 for M67 and 0.7 or fainter for NGC 752. Main-sequence fitting to the theoretical isochrones of Ciardullo and Demarque (1977) (Yale isochrones) with the appropriate metallicity and $Y = 0.30$ produces absolute visual magnitudes for the clump of 0.5, 0.8, and 0.8 for NGC 2204, NGC 2420, and NGC 2506 respectively. (See the Appendix for cluster references.) These should be regarded as less certain because they are tied to a specific set of theoretical models and $Y = 0.3$. They are, however, consistent with a Hyades modulus of 3.3 (Anthony-Twarog and Demarque 1977).

Given the age (see discussion below) and metallicity of NGC 188 and NGC 6791, the clump data indicate an absolute magnitude for these clusters of 0.8 or fainter. The clump of NGC 188 is at $V = 12.4$, while that of NGC 6791 is at $V = 14.7$ (KI), or $M_v = 1.1$ for NGC 188 and 1.2 for NGC 6791, using the moduli derived above.

The alternate approach is a direct comparison of the clusters with theoretical isochrones, providing age and distance simultaneously. Two problems arise: (i) one must assume an absolute value for the helium abundance, in addition to a relative cluster Y, and (ii) two sets of theoretical isochrones exist (Yale isochrones, VandenBerg 1983, hereafter VB) which imply different ages and distances for the same clusters. We will discuss the clusters using each set of models first, and return to the helium question last.

A comparison of the Yale isochrones of $Y = 0.30$ and $Z = 0.019$ with NGC 6791 is shown in Figure 4. ($Y = 0.3$ has been chosen to allow direct comparison with similar isochrone fits for other clusters.) The isochrones have been reddened by $E(B-V) = 0.20$, and an apparent modulus of 13.5 has been adopted. The unevolved main-sequence fit is quite good, but this is not unexpected. The modulus is tied differentially to NGC 188, and, as discussed earlier, the modulus of NGC 188 has been adjusted to $(m-M) = 11.3$ to guarantee an equivalent fit of the isochrones and the normal points of NGC 188.

The cluster age is estimated at $6.0 \pm 0.7 \times 10^9$ yr, based on the fit of the isochrones to the color of the turnoff, the same technique applied to all the clusters in the Appendix. This should produce a reliable relative age sequence for all the clusters. While there is little doubt that NGC 6791 is older than NGC 188, just how much older is in question. If the metallicity were significantly lower than assumed, or the $(B-V)$ colors were too blue due to an error in the assumed reddening or the zero point of the photometric calibration, or both, the age
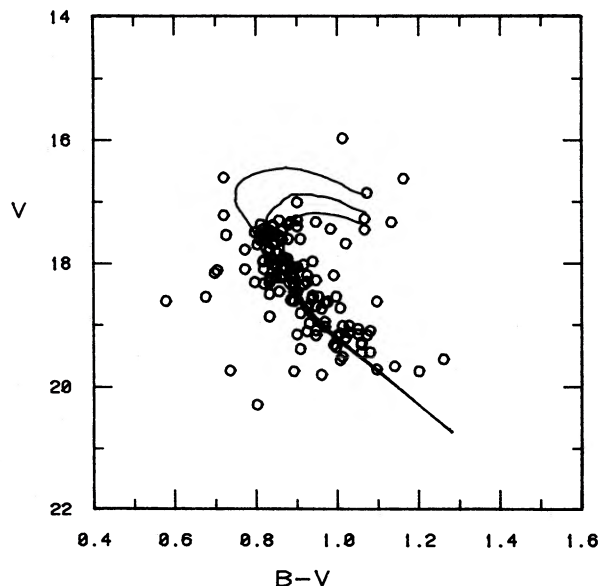

FIG. 4.—Comparison of data in Table 2 with theoretical isochrones of Ciardullo and Demarque 1977. The isochrones have been reddened by $E(B-V) = 0.20$ and a distance modulus of $(m - M) = 13.5$ adopted. Models have $(Y, Z) = (0.3, 0.019)$ and ages of 4, 6, and 8×10^9 yr.

estimate would increase proportionately (by $\sim 2 \times 10^9$ yr for a color error of 0.05 mag). As a secondary check on the age estimate, a technique based on the cm–diagram morphology and independent of the reddening has been devised; the explanation and calibration of the technique are detailed in the Appendix. In short, a parameter called the Morphological Age Ratio (MAR) is computed from the relative position of the giant branch and the cluster turnoff. The MAR is a direct measure of the age with only a weak apparent dependence upon metallicity. The MAR for NGC 6791 is 4.0 ± 0.2, leading to an age of $5.6 \pm 0.3 \times 10^9$ yr, or roughly midway between NGC 188 and Melotte 66. Note that the absolute scale for the ages is tied to the Yale isochrones with $Y = 0.3$. Lowering the helium abundance to $Y = 0.2$ will lead to an increase of 10% to 20% in the ages and approximately 0.3 in the distance moduli.

The alternate set of theoretical models is those of VB, where the dominant differences from the Yale models are due to a more comprehensive treatment of the mixing-length parameter. The main-sequence fit to the isochrones of VB is shown in Figure 5, where the $Y = 0.20$, $Z = 0.0169$ composition has been chosen because VB finds that this provided an optimum match to NGC 188 compared to $Y = 0.30$ when $(m - M) = 11.1$ is adopted; the age derived from this comparison is $12 \pm 1 \times 10^9$ yr, again fitting primarily to the color of the turnoff. It should be noted that a possible point of confusion arises in the discussion of VB. For NGC 188, VB derived an apparent modulus of 11.1 based on a fit of the cluster cm diagram to his isochrones, in apparent agreement with the results of Demarque and McClure (1977) as listed in Table 4 of VB. In reality, 11.1 is the true modulus derived by Demarque and McClure (1977). Thus, the modulus for NGC 188 derived by VB is 0.3 mag smaller than that produced by comparison to the Yale isochrones, identical to the differential in a comparison of the data for NGC 6791; from Figure 5 the VB modulus for NGC 6791 is only 13.2.

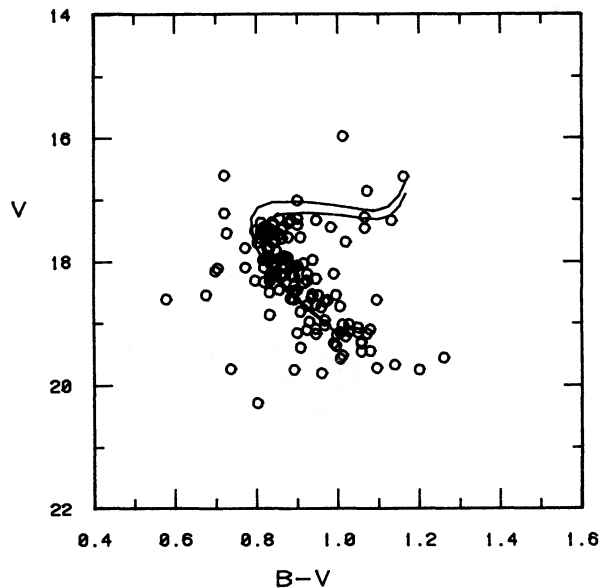It must be concluded that, after adjustments are made to fit

FIG. 5.—Same as Fig. 4 but with isochrones of VandenBerg 1983. Distance modulus of $(m - M) = 13.2$ has been adopted. Models have $(Y, Z) = (0.2, 0.0169)$ and ages of 10 and 12×10^9 yr.

the cluster main sequences with isochrone sets of the same Z, the models of VB imply moduli which are systematically smaller by 0.2 mag than those of the Yale isochrones, a result confirmed by direct comparison of the main sequences of VB for $Y = 0.2$ with the Yale isochrones for $Y = 0.3$. Note that the correction in the distance moduli for the differences in Z (0.0169 for VB, 0.019 for Yale) has decreased the discrepancy from 0.3 to 0.2 mag.

But what about the helium difference? Unfortunately, any attempt to lower the helium abundance of the Yale models or raise that of the VB models, or both, only makes matters worse. For example, if a direct comparison were made with the VB models of $Y = 0.30$, the cluster moduli would decrease by an additional 0.3 mag, leading to a 0.5 mag disagreement.

Given that the different isochrones produce different moduli, which set provides the more reliable distances to the clusters? While there is little disagreement that $Y = 0.20$ models for either set of isochrones provide better fits to NGC 188 (TW; VB), and that the VB isochrones match the cm–diagram morphology better, there are currently no definitive tests of the reliability of the distance scale provided by either. The key stumbling block is our lack of understanding of the relative helium abundances in the clusters. The only object for which a consensus of opinion exists regarding the mass fraction of the helium content is the Sun, where most models predict $Y = 0.24 \pm 0.02$ (See VandenBerg and Bridges 1984 for a thorough discussion of the helium abundance question.) for globular and open clusters, field stars, and planetary nebulae, the common range of values is $Y = 0.20$–0.33, with an indication that Y and Z are correlated (e.g., Perrin et al. 1977; Peimbert and Serrano 1980). This trend has been supported by observations of extragalactic H II regions (Lequeux 1979; Talent 1980) and implies that the old disk and globular clusters should have Y less than the solar value. This claim has been seriously challenged by the recent work of Kunth and Sargent (1983), who find no statistically significant trend of Y with Z among the observations of extragalactic H II regions.

The current uncertainty in the choice of cluster-distance

scales underscores the importance of the answer for a number of fundamental astrophysical questions. As an example, if the VB isochrones are correct and we adopt $Y = 0.25$, the apparent modulus for NGC 6791 is lowered to 13.1, and the red-giant clump has an absolute visual magnitude of $+1.6$. Because of their greater age, i.e., lower mass, the metal-rich RR Lyrae stars should have M_v equal to or fainter than this. If the absolute magnitude of the clump in 47 Tuc is $+0.9$, the sensitivity of the horizontal-branch luminosity to metallicity must be significantly larger than expected from theory (Iben 1974). While Sandage (1982) finds an apparent strong correlation between horizontal branch luminosity and metallicity, with 47 Tuc having $M_v \approx 1.2$, the direct metallicity effect is claimed to be negligible. The cause of the apparent correlation is the helium abundance, with Y and Z anticorrelated. The faint luminosity for the NGC 6791 clump is consistent with the apparent trend, but sheds no light on its ultimate cause. If this apparent strong correlation between luminosity and metallicity is universal, whatever its source, the implication for the distance to the Galactic center, supposedly a very metal-rich region based upon the distribution of RR Lyrae stars, is one obvious example of why the absolute scale of open-cluster distances is important. If the open clusters have similar helium abundances, the moduli based on either set of models would indicate that the claim of a constant red-giant–clump magnitude for clusters older than the Hyades (Cannon 1970) was premature. The clump appears to grow significantly fainter with increasing age (or higher metallicity, or both) for clusters as old as NGC 6791. Resolution of these questions will have to await further observations.

IV. NGC 6535

a) Reduction and Calibration of Data

The globular cluster field in NGC 6535 is significantly more crowded than NGC 6791, and hence an aperture photometry algorithm such as the Mountain Photometry Code is inappropriate. In 1983 May, the Kitt Peak Interactive Picture Processing System RICHFLD program was used to process the frames in NGC 6535. The frames were previously corrected for geometric distortion in a batch process on the Kitt Peak Cyber computer.

The RICHFLD photometry system operates on undistorted image frames by scaling the intensity profile of each star to a point spread function (psf) constructed from the cleaned images of several relatively bright stars. An auto-scaling algorithm finds, by χ^2 fitting, the center of the star within a small subraster of points, then finds the local planar sky level and the scaling ratio r, rejecting noisy pixels in the sky. The logarithm of the scaling ratio yields the magnitude relative to the adopted magnitude of the psf, and the statistical error of the scaling ratio, ϵ_r, yields the error in the instrumental magnitude $\sigma_m = (1.086) \epsilon_r/r$. These formal magnitude errors derived from the scaling ratio are typically 0.01 mag for stars with $V \leq 20$ on 1981 September 2, with somewhat higher errors (0.04) for stars of comparable brightness on the night of poorer seeing, 1981 September 5. Formal color errors are typically 0.01 mag for the September 2 estimates, and reach ~ 0.05 for the September 5 measurements. These formal errors are very likely underestimates of the true instrumental magnitude errors and will be used only for comparison and weighting.

The survey field in NGC 6535, which includes part of the center and an area southeast of the center, is shown in Figure 6; a number of stars in LI's photographic survey are included,
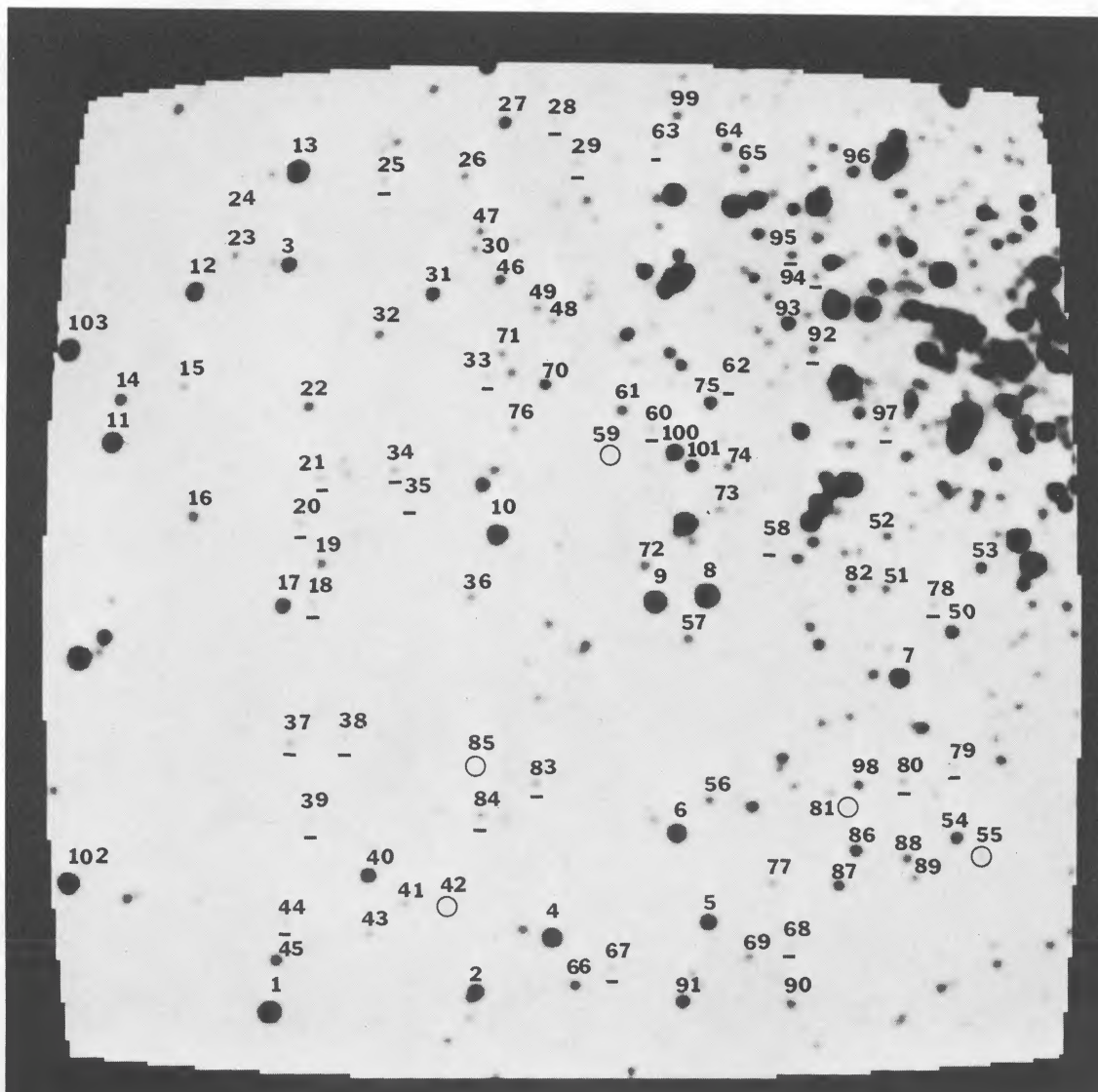
FIG. 6.—Identification chart for NGC 6535, made from a blue Video Camera frame. Numbers are on system of current investigation. Cross-identification with system of Liller 1980 can be found in Table 3. Field is approximately 3′ across, with north up, east to the left.

as well as one pe-sequence star, L94. As for NGC 6791, a simple linear form of the magnitude and color calibration has been employed for which only the zero-point correction terms must be obtained. We have elected to employ the pe value for L94 only to establish the zero points of the calibration. The photometry so calibrated is listed in Table 3, where the entries in column (6) indicate whether values from both Nights 1 and 3 are included, and column (7) notes identifications on LI's numbering scheme. The values listed are weighted means, using the individual instrumental magnitude error and derived instrumental color errors as weights. The errors listed with the photometric values are derived only from the comparison of

values for the two nights' measurements. It may be noted that the derived magnitude and color for L24 are widely discrepant with respect to LI's photographic values. The formal error for the one Video Camera instrumental V magnitude is quite large, and it must be assumed that the present photometry for this star is in error and unusable. A cm diagram of these photometric values is shown in Figure 7. The large scatter near the turnoff compared to that found in the photometry of NGC 6791 is the result of the fainter magnitude of the turnoff, greater crowding in the globular cluster, and the lower quality of the sky conditions during the observations of NGC 6535.

One reason not to use the additional information provided

TABLE 3

VIDEO CAMERA PHOTOMETRY IN NGC 6535

	V	σ_V	$B-V$	σ_{B-V}	Nights[a]	Identification		V	σ_V	$B-V$	σ_{B-V}	Nights[a]	Identification
1......	16.04	0.00	1.18	0.00	1, 3	L94	53......	18.75	...	0.99	...	1	...
2......	17.54	...	1.21	...	1	L73	54......	18.65	...	0.98	...	1	...
3......	17.91	...	1.34	...	1	L50	55......	20.31	...	0.80	...	1	...
4......	16.80	0.01	1.11	0.05	1, 3	L72	56......	19.33	0.01	0.92	0.08	1, 3	...
5......	17.79	0.00	1.01	0.01	1, 3	L47	57......	19.26	0.07	0.92	0.06	1, 3	...
6......	17.18	0.02	0.98	0.02	1, 3	L48	58......	20.38	0.48	0.88	0.63	1, 3	...
7......	16.86	...	1.06	...	1	L23	59......	20.65	...	1.09	...	1	...
8......	16.67	...	−0.08	...	1	L24	60......	20.10	0.58	0.81	0.94	1, 3	...
9......	16.79	0.01	0.39	0.03	1, 3	L25	61......	19.15	0.06	0.83	0.07	1, 3	...
10......	16.61	0.02	1.13	0.02	1, 3	L49	62......	20.63	0.15	0.84	0.06	1, 3	...
11......	16.65	0.01	1.02	0.00	1, 3	L74	63......	20.25	...	0.90	...	1	...
12......	17.20	0.03	1.09	0.01	1, 3	L76	64......	19.03	...	0.94	...	1	...
13......	16.71	...	0.33	...	1	L51	65......	19.20	...	0.88	...	1	...
14......	18.42	0.00	1.28	0.04	1, 3	...	66......	18.89	0.05	0.94	0.03	1, 3	...
15......	19.59	0.07	1.01	0.08	1, 3	...	67......	20.00	0.06	0.90	0.21	1, 3	...
16......	19.03	0.01	0.85	0.02	1, 3	...	68......	20.42	0.01	0.65	0.34	1, 3	...
17......	17.86	0.01	1.06	0.06	1, 3	...	69......	19.35	0.04	1.24	0.03	1, 3	...
18......	19.89	0.05	0.99	0.08	1, 3	...	70......	18.86	0.02	0.83	0.05	1, 3	...
19......	19.18	0.04	0.89	0.08	1, 3	...	71......	19.76	...	0.68	...	1	...
20......	19.96	0.02	0.80	0.12	1, 3	...	72......	19.17	0.06	0.98	0.05	1, 3	...
21......	20.04	0.05	0.62	0.15	1, 3	...	73......	19.71	0.08	0.92	0.12	1, 3	...
22......	19.07	0.02	0.88	0.04	1, 3	...	74......	19.40	0.07	0.82	0.10	1, 3	...
23......	19.57	...	0.88	...	1	...	75......	18.46	0.07	0.82	0.06	1, 3	...
24......	20.21	...	1.06	...	1	...	76......	19.62	0.00	1.00	0.04	1, 3	...
25......	20.08	...	0.78	...	1	...	77......	19.72	0.08	0.93	0.09	1, 3	...
26......	19.70	...	0.79	...	1	...	78......	20.12	...	0.79	...	1	...
27......	18.73	...	0.83	...	1	...	79......	19.05[c]	...	...	...	1	...
28......	20.55	...	0.83	...	1	...	80......	19.64	...	1.08	...	1	...
29......	20.24	...	0.69	...	1	...	81......	20.18	...	0.85	...	1	...
30......	19.81	...	0.74	...	1	...	82......	19.27	...	0.86	...	1	...
31......	18.25	...	1.21	...	1	...	83......	19.57	0.02	1.03	0.02	1, 3	...
32......	19.34	0.02	0.80	0.03	1, 3	...	84......	19.40	0.09	1.21	0.13	1, 3	...
33......	20.10	...	0.72[b]	0.02	1, 3	...	85......	20.44	0.19	0.94	0.10	1, 3	...
34......	19.79	0.07	0.80	0.23	1, 3	...	86......	18.53	0.02	0.99	0.04	1, 3	...
35......	20.56	0.04	0.73	0.00	1, 3	...	87......	18.75	0.03	−1.90	1.43	1, 3	...
36......	19.54	0.02	0.95	0.12	1, 3	...	88......	19.27	...	0.82	...	1	...
37......	19.79	0.05	0.91	0.04	1, 3	...	89......	19.60	...	0.84	...	1	...
38......	19.94	0.07	0.10	0.16	1, 3	...	90......	19.18	0.05	0.91	0.10	1, 3	...
39......	20.51	...	0.41	...	1	...	91......	18.30	0.00	1.02	0.05	1, 3	...
40......	17.91	0.02	1.15	0.01	1, 3	...	92......	19.35	0.14	0.93	0.15	1, 3	...
41......	19.67	0.04	0.95	0.12	1, 3	...	93......	18.21	...	1.10	...	1	...
42......	20.44	0.08	0.99	0.26	1, 3	...	94......	19.66[c]	...	...	...	1	...
43......	19.63	0.00	2.41	0.73	1, 3	...	95......	19.20	...	1.16	...	1	...
44......	20.16	0.01	0.86	0.04	1, 3	...	96......	18.94	...	0.64	...	1	...
45......	18.57	0.13	1.18	0.02	1, 3	...	97......	19.88	...	0.98	...	1	...
46......	19.10	0.04	0.90	0.04	1, 3	...	98......	19.00	...	1.01	...	1	...
47......	19.58	...	0.77	...	1	...	99......	19.36	...	0.81	...	1	...
48......	19.74	0.08	0.99	0.10	1, 3	...	100......	17.70	...	1.02	...	1	...
49......	19.64	0.05	0.85	0.00	1, 3	...	101......	18.52	...	0.95	...	1	...
50......	18.27	...	1.11	...	1	...	102......	15.90	...	1.62	...	3	L95
51......	19.54	...	0.69	...	1	...	103......	16.01	...	1.50	...	3	L75
52......	19.44	...	0.79	...	1	...							

[a] Night 1 = September 2, Night 3 = September 5.
[b] B magnitude from Night 1 only.
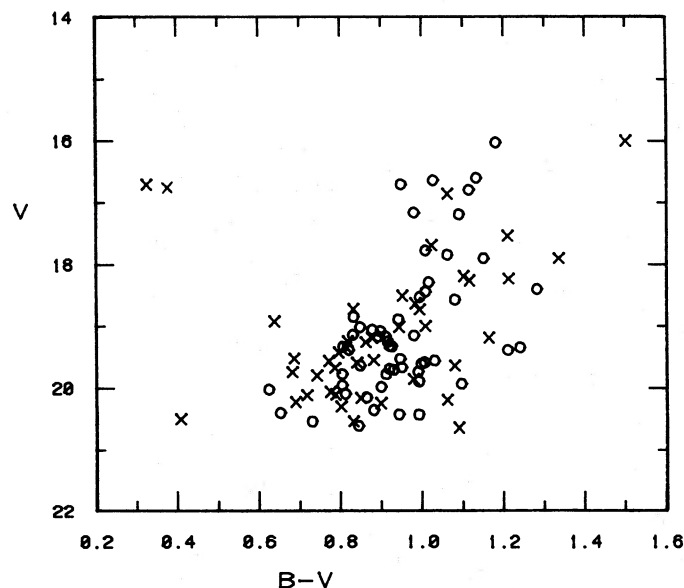[c] V magnitude from Night 1 only.

FIG. 7.—Color-magnitude diagram for NGC 6535 using data of Table 3 based on Video Camera photometry. Open circles are observations averaged over two nights, crosses represent single observations.

TABLE 4

A. COMPARISON OF LILLER'S PHOTOGRAPHIC VALUES
AND VIDEO CAMERA VALUES

Star	V_{vc}	$\delta(V_{vc} - V_{pg})$	$\delta(B-V)_{vc-pg}$
L23..........	16.86	+0.04	+0.01
L25..........	16.79	−0.05	+0.14
L47..........	17.79	−0.15	+0.27
L48..........	17.18	−0.12	+0.18
L49..........	16.61	+0.04	+0.06
L50..........	17.91	−0.11	+0.31
L51..........	16.71	−0.10	+0.10
L72..........	16.80	−0.07	+0.09
L73..........	17.54	−0.12	+0.16
L74..........	16.65	−0.06	+0.11
L76..........	17.20	−0.13	+0.21
L75..........	16.01	+0.10	−0.06
L94..........	16.04	0.00	−0.02
L95..........	15.90	+0.07	−0.08

B. COMPARISON OF LILLER'S PHOTOGRAPHIC
AND PHOTOELECTRIC VALUES

Star	V_{vc}	$\delta(V_{vc} - V_{pg})$	$\delta(B-V)_{vc-pg}$
L58..........	14.48	+0.07	−0.06
L70..........	15.40	+0.01	+0.01
L86..........	16.85	+0.05	+0.11
L89..........	16.78	−0.06	+0.11
L94..........	16.04	0.00	−0.02
L102........	16.23	0.00	+0.01
L103........	16.25	+0.01	−0.08

by stars in the field with photographic measurements from LI is the presence of a magnitude-dependent error in the photographic magnitudes and colors. This systematic trend is indicated by a comparison of our vc data with LI's photographic (pg) data for 14 stars in common, and a comparison of LI's pe data with her own pg results for seven stars. The one star common to both comparisons is L94, used to zero-point the vc data. The uncertainty in the vc photometric zero points due to the combined uncertainty of LI's pe value and the vc magnitudes is ± 0.04 mag for both V and $B-V$. The combined presentation of the two comparisons, pe with pg and vc with pg, confirms our assumption that the relationship between vc and pe magnitudes is linear and that the vc photometry has been reliably (within ± 0.04) transferred to the pe system of LI. Table 4 presents the comparison of pg values with vc data and pg values with LI's pe results, with a graphic illustration given in Figure 8. Open circles are (pg − pe) versus V_{pe}, while closed circles are (vc − pg) versus V_{vc} for V and $B-V$ comparisons. The small dispersion in the color residuals implies that the vc colors are internally precise to ± 0.03 to 0.04 down to $V = 18$.

While these comparisons demonstrate the existence of a magnitude-dependent error in the pg values of LI for $V \geq 16$, the origin of the problem is a bit hard to unravel. Much of it is undoubtedly due to the use of a sequence-extending wedge coupled with measurements on an iris photometer, a combination which is known to produce magnitude-dependent errors (cf. Blanco 1982). An additional problem may be the lack of application of a color term by LI, since significant effects are usually found for V magnitudes derived from D plate/GG-495 filter combinations (e.g. McClure, Twarog, and Forrester 1981).

b) *Analysis and Discussion of the Photometric Results*

In her photometric analysis of NGC 6535, LI employed Harris's (1976) estimate of 0.36 for the reddening for the cluster, noting its consistency with a value of 0.33 derived from a comparison of the observed color of the blue edge of the instability strip and Sandage's (1969) value of 0.18 for this parameter. The

reddening maps of Burstein and Heiles (1982) may also be consulted; at the position of NGC 6535 of $(l, b) = (27.2°, 10.4°)$, a value of $E(B-V) = 0.37 \pm 0.04$ is indicated. LI's adopted value of $E(B-V) = 0.36$ will be used in the following discussion.

We have also followed LI's discussion of the distance to NGC 6535, based on a comparison of the horizontal branch at
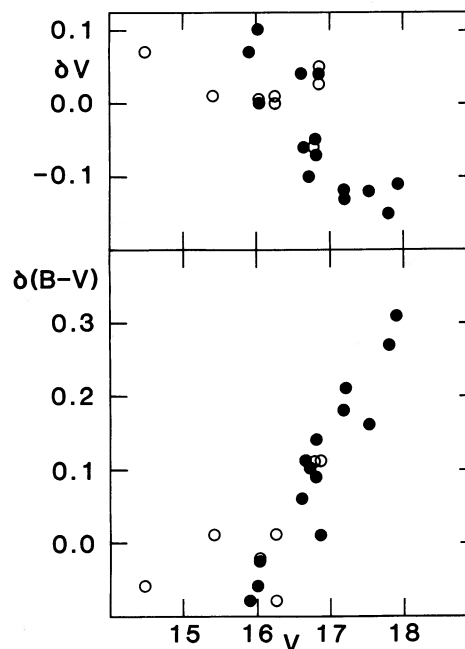

FIG. 8.—Differences in V and $(B-V)$ between photographic data of Liller 1980 and Video Camera data of current investigation (*closed circles*) and between photographic and photoelectric data of Liller (1980) (*open circles*) in the sense (Video Camera − photographs) vs. Video Camera V, and (photoelectric − photographic) vs. V_{pe}.

$V = 15.8 \pm 0.1$, and an absolute magnitude of 0.6 for the horizontal branch. A true distance modulus of 14.0 is derived, if a ratio of $A_v/E(B-V)$ of 3.2 is used. LI also notes the similarity of NGC 6535's essentially absent red horizontal branch and sloping blue horizontal branch to that of M13, which has a metallicity of [Fe/H] ~ -1.4 (e.g. Pilachowski 1984).

An age estimate based on comparison of the color-magnitude diagram with theoretical isochrones is not possible due to the large spread in $(B-V)$ near the turnoff. The turnoff magnitude of $V = 19.0$ is 3.2 mag fainter than the magnitude of the horizontal branch, indicating a typical globular cluster age; this would imply an age of $15\text{--}18 \times 10^9$ yr on VB's scale.

Returning to the original question of interest regarding NGC 6535, there is little evidence for a significant population of blue stragglers, even in the central areas of the cluster. From Figure 9, one would estimate that at most two stars lie in positions consistent with probable blue-straggler status, and these are only slightly above the turnoff. While photometric uncertainty is a problem, its effect is much more noticeable on $(B-V)$ than on V, so it is unlikely that true stragglers have been shifted toward fainter magnitudes and an apparently normal position on the main sequence by incorrect photometry. If globular-cluster production is similar to that in old open clusters, the number of blue stragglers should be 5%–10% of the number of stars near the turnoff; for NGC 6535, this implies two to five stragglers. Without cluster membership information and better photometry, the best one can say is that the number of blue stragglers in NGC 6535 is not significantly greater than expected by comparison with old open clusters, and may be zero.

V. CONCLUSIONS AND FUTURE RESEARCH

Video Camera photometry obtained with the KPNO 2.1 m telescope has been reduced and analyzed for two clusters, an old open cluster, NGC 6791, and a globular cluster, NGC 6535. For NGC 6791, the conclusions are:

1. In contradiction to the photographic data of KI, the cm diagram near the turnoff bears a striking similarity to that of NGC 188, with NGC 6791 appearing older. The cm–diagram morphology allows one to infer that the two clusters are also similar in metallicity, in agreement with recent photometric results.

2. A rediscussion of the cluster reddening leads to an adopted value of $E(B-V) = 0.20 \pm 0.02$, significantly larger than that adopted by Harris and Canterna (1981). Comparison of the cm diagram with theoretical models using this reddening indicates an age intermediate between NGC 188 and Melotte 66 (6×10^9 yr for the Yale models, 12×10^9 yr for VB), consistent with the ranking of their MARs (see Appendix). Adoption of a lower reddening would lead to a significantly greater age, though such a possibility cannot be excluded given current uncertainties in the cluster parameters.

3. Independent of the zero point of the scale, the apparent modulus of NGC 6791 is 2.2 mag larger than that of NGC 188, assuming that the reddening and metallicity adopted are correct. If $(m - M) = 11.3$ for NGC 188, $(m - M) = 13.5$ for NGC 6791, assuming that both clusters have the same helium abundance as the Hyades. Use of these models implies $M_v = 1.1\text{--}1.2$ for the red-giant clump, indicating a significant age dependence for the absolute magnitude of this feature in open clusters as old as NGC 6791 and, indirectly, a strong metallicity dependence for the absolute magnitude of the horizontal branch.

4. The size of the metallicity effect on the horizontal branch is tied to the choice of theoretical models and the difference in helium abundance among the clusters. For the same Y and Z, use of the isochrones of VB at the metal-rich end of the scale produces distance moduli which are approximately 0.5 mag smaller than the Yale isochrone fits, implying that the clump
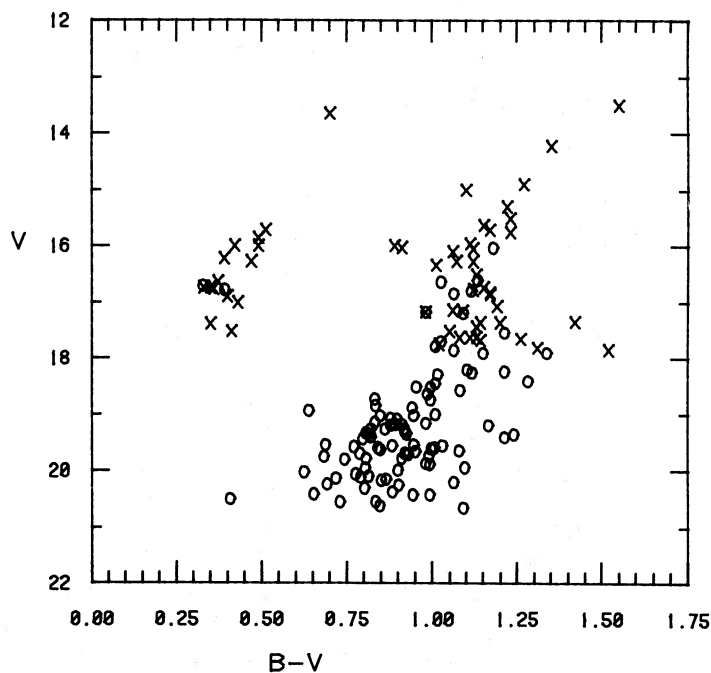

FIG. 9.—Color-magnitude diagram of NGC 6535. Open circles are data from Table 3; crosses are the results of Liller 1980 within 90″ of the cluster center, with a correction applied to stars with $V > 16$ based on the linear-magnitude–dependent errors in V and $B - V$ described in the text and illustrated in Fig. 8.

M_v in NGC 6791 could be as faint as 1.8 for a high helium abundance of $Y = 0.3$. If older clusters have correspondingly lower Y, part of the age dependence of the clump luminosity could be removed.

For NGC 6535, the conclusions are:

5. The cm–diagram morphology indicates a cluster very similar to M13. Based on the relative magnitudes of the horizontal-branch and main-sequence turnoff, the age is comparable to other typical globular clusters, or approximately $15–18 \times 10^9$ yr on the VB scale of ages.

6. The sparse field in the cluster allowed photometry close to the core of the cluster. Though the statistics are poor, there is no evidence for a significant population of blue stragglers. At best, the number of possible candidates is typical of what is found in old open clusters; at worst, no likely blue straggler candidates exist.

7. The photographic data of LI appear to suffer from a magnitude-dependent error, probably the result of using a wedge-extended calibration sequence.

In regard to future research, the uncertainties generated in the discussion of NGC 6791 point to a number of very obvious, but crucial, programs for clarifying some of these questions. A direct determination of the reddening and metallicity by spectroscopic or photometric means or both would permit significantly tighter constraints on the age and distance. Better photometry of the giant branch would also focus on the reality of the broad spread in color found among the giants in the cm diagram of KI, a point not discussed in this paper. A similar scatter below the red-giant clump exists in NGC 188 and may reflect a transition toward greater complexity in evolution among lower-mass stars, as evidenced by recent work on abundance variations in globular clusters. Both programs would be aided greatly by a proper-motion membership study to separate cluster stars from the rich field distribution; such a survey is planned (Anthony-Twarog and Cudworth 1984, private communication).

Finally, the continuing value of testing the effects of metallicity and age on the horizontal-branch luminosity open-cluster cm diagrams cannot be overlooked. While the question of the relative helium abundances may never be solved, for an assumed absolute Y based on the Sun or model-fitting to stars with well-determined parallaxes and known metal abundance, an internally consistent set of moduli and ages should be derivable for any set of isochrones. If the primary need for faint, high-accuracy, main-sequence photometry is satisfied, systematic differences of 0.3 to 0.4 mag in the red-giant–clump luminosity should be detectable. Such data would allow strong constraints to be placed on the upper limits of the luminosity of the metal-rich RR Lyrae stars and significantly influence our understanding of the horizontal branches of clusters poorer in metals.

APPENDIX

I. THE TECHNIQUE

Over the years, a number of attempts have been made to use cm–diagram morphology to rank clusters in either age or metallicity. For the globulars, where age variation may be small, reddening-dependent parameters such as $(B-V)_{0g}$ (Sandage and Wallerstein 1960) and reddening-free measures like S (Hartwick 1968) and $D(B-V)$ (KI 1965) have been used as metallicity indicators. Similar approaches have been adopted for open clusters, for which age is widely variable. For clusters older than the Hyades, age estimates have been based upon ΔV, the difference in magnitude between the red-giant clump (Cannon 1970) and a point near the main-sequence turnoff (e.g., Hawarden 1971) and/or $\Delta(B-V)$, the difference in color between the giant branch and the cluster turnoff (e.g., Christian and Janes 1979).

While such indices are designed to be insensitive to reddening, the same cannot be said with respect to metallicity. However, a check of theoretical isochrones (Ciardullo and Demarque 1979) covering the range in age and metallicity normally found among Galactic open clusters reveals that metallicity effects on both types of indices affect the ages in the same sense. We have therefore derived a new parameter, the MAR, defined as $\Delta V / \Delta(B-V)$, where ΔV is the difference in magnitude between the red-giant–branch clump and the brightest point of the cluster turnoff, and $\Delta(B-V)$ is the difference in color between the bluest point of the cluster turnoff and the color of the red-giant branch at the level of the red-giant clump. The values of such a ratio are that it is reddening free; it makes maximum use of the age effect on both variables, because ΔV increases while $\Delta(B-V)$ decreases with increasing age; and it significantly reduces, but does not eliminate, the metallicity effect.

For calibration purposes, we have collected information on seven clusters older than the Hyades. They have been chosen because they all have reliable main-sequence photometry and all but one have accurate giant-branch data. (The one exception, NGC 2204, will be discussed in more detail below.) They all have reddening and metallicity estimates based on UBV, DDO, or $uvby$ Hβ photometry. Finally, age estimates based on main-sequence fitting to an internally consistent set of theoretical isochrones are available. The specific information for each cluster is found in Table 5.

Before we discuss individual clusters, a few points are in order. First, the choice of a particular set of theoretical isochrones to calibrate the cluster ages is an arbitrary one. Our purpose is to demonstrate that the MAR provides a reliable age ranking of the cluster; the absolute scale will differ according to the choice of theoretical models adopted and will undoubtedly change as stellar evolution theory evolves an improves in the future.

Second, for clusters younger than 10^9 yr, the location of the red-giant clump and the exact position of the turnoff luminosity become increasingly difficult to identify. The absolute magnitude of the clump also brightens for younger clusters, negating the age

TABLE 5
CLUSTER PARAMETERS FOR MAR CALCULATIONS

Cluster	$E(B-V)$	$[Fe/H]_{Hy}$	Age ($\times 10^9$ yr)	$(B-V)_{to}$[a]	V_{to}[a]	$(B-V)_g$	V_g	MAR
NGC 188	0.08	−0.25	5.0 ± 0.7	0.67	14.80	1.32	12.35	3.77
NGC 752	0.04	−0.35	2.2 ± 0.2	0.40	9.95	1.05	9.00	1.46
NGC 2204	0.08	−0.55	2.5 ± 0.3	0.36	15.40	1.24	13.80	1.82
NGC 2420	0.02	−0.60	3.8 ± 0.5	0.40	14.25	1.08	12.55	2.50
NGC 2506	0.05	−0.65	3.4 ± 0.5	0.39	14.80	1.05	13.20	2.42
M67	0.05	−0.20	4.0 ± 0.5	0.56	12.55	1.16	10.55	3.33
Melotte 66	0.14	−0.65	6.5 ± 0.7	0.66	16.70	1.17	14.50	4.33

[a] Subscript "to" refers to "turnoff"; no reddening correction has been applied.

sensitivity of the MAR. The calibration should not be applied to clusters with ages less than 10^9 yr. The color difference $\Delta(B-V)$ has long been known to increase dramatically with age for younger clusters and can be adopted. Additionally, age estimation should not be extrapolated beyond the last calibration cluster, Melotte 66, because of the current lack of knowledge regarding the linearity beyond this point.

Third, different observers will often derive different estimates of the same parameter using the same observational data unless explicit comparisons with the standard calibrators are possible. To minimize this problem, the exact positions of the various features used to estimate the MAR for each cluster are listed in Table 5. Two possible areas of confusion are the color of the giant branch and the luminosity of the turnoff.

The color of the giant branch should not be identified as the color of the red-giant clump. In most clusters, there is a gap of a few hundredths of a magnitude in $(B-V)$ between the clump and the red-giant branch. (One possible extreme example of this will be mentioned below, NGC 2204.) Use of the red-giant clump $(B-V)$ will lead to an overestimate of the age of the cluster.

In most clusters, the brightest point at the turnoff is easily identified. However, with the metal-poor, anticenter clusters (e.g. NGC 2420, NGC 2506) some ambiguity is present because of the existence of a small band of stars located 0.5 to 0.7 mag above the turnoff. Whether these are binaries or stars in a rapid phase of post–main-sequence evolution is unknown (McClure, Twarog, and Forrester 1981). Because of their typically small numbers and their poorly understood evolutionary state, these stars have been ignored in pinpointing the location of the brightest level at the turnoff for the clusters NGC 2204, NGC 2506, NGC 2420, and Melotte 66.

Finally, the calibration is based solely upon Galactic open clusters. Because there is a general correlation of metallicity and age in the disk as a result of the chemical history of the Galaxy, not all combinations of age and metallicity space can be tested. The calibration is therefore unique to our Galaxy and should not be applied, for example, to the Magellanic Clouds until reliable age and metallicity estimates for clusters in these galaxies become available.

The age—MAR data of Table 5 are plotted in Figure 10. Uncertainties in the estimation of the MAR are quite stable over the entire age range, at values between 0.2 and 0.3. The two exceptions, NGC 2204 and Melotte 66, will be discussed below.

Because of the small number of clusters and the uncertainty of the data, a simple linear relation was drawn by eye through the data:

$$t_9 = 1.4 \text{ MAR},$$

where t_9 is the age in 10^9 yr.

FIG. 10.—Calibration of MAR with known ages of well-defined clusters. Solid line is a visual fit to the data defined by the relation $t_9 = 1.4$ MAR.

II. THE CLUSTER DATA

For each of the clusters listed in Table 5, the sources of the parameters will be given below, along with an explanation of any changes from the published values. In all instances, [Fe/H] is defined as $\log (Fe/H)_{\rm cluster} - \log (Fe/H)_{\rm Hyades}$, a choice made because most photometric metallicity indicators are zeroed with respect to the Hyades. In all cases but one, [Fe/H] is a direct average of the metallicity based on DDO and *UBV* photometry; NGC 752 includes *uvby* Hβ. The [Fe/H] values of Table 5 are given to the nearest 0.05 dex and have a typical standard error of the mean near ± 0.1 dex. Two clusters, M67 and NGC 2420, have been involved in the recent controversy over the metallicity scale deduced from echelle spectroscopy versus that from photometry. Since only photometric abundances are used in the present investigation, the values of Table 5 are effectively on the old system. It is assumed that all clusters have the same helium abundance.

Note that the references given below are not meant to be comprehensive. In most instances, the age, metallicity, and reddening are derived in the same paper where a more detailed discussion of previous work on these parameters may be found. To reiterate, our approach has been to maintain internal consistency whenever possible; changes in the slope and zero point of the calibration are likely as theory and observation evolve, but the relation ranking should be reasonably stable.

NGC 188.—Reddening and metallicity: Eggen and Sandage (1969), McClure (1974); cm diagram: McClure and Twarog (1977), Twarog (1983*a*); age: TW.

The significant change from earlier work is the increase in age for NGC 188 from 4.5×10^9 yr to 5.0×10^9 yr. The former value is based upon a differential comparison of the cm diagram of M67 and NGC 188 by TW. In all instances in that investigation, cluster parameters were selected to minimize the difference in position between the giant branches of the two clusters. Therefore, it was assumed that M67 and NGC 188 has the same metallicity at a value higher than solar. As noted in the discussion of M67 below, the best estimate for this cluster is solar or less, and NGC 188 appears to have a slighly lower metallicity than M67. To account for this, the age of NGC 188 has been increased.

NGC 752.—Reddening, metallicity, age: Twarog (1983*b*); cm diagram: Johnson (1953), Eggen (1963).

The principal source of uncertainty for this cluster is the small number of cluster members. The giant branch is poorly defined, though a clump of stars does appear near $V = 9.0$. $(B-V)_{\rm g}$, however, is defined as the color of the giant branch at this level. The reddest star at the magnitude level of the clump has $(B-V)$ at 1.05, the value adopted in Table 5. Since the giant branch is normally a few hundredths of a magnitude redder than the clump, this color should be regarded as a lower limit and the MAR determination an upper limit for the cluster's age.

NGC 2204.—Reddening and metallicity: Hawarden (1976*a*), Dawson (1981); age: Frogel and Twarog (1983); cm diagram: Hawarden (1976*a*), Frogel and Twarog (1983).

This cluster is the least reliable point in the calibration. While the turnoff characteristics are accurately determined, the giant branch is ill defined. From Figure 2 of Hawarden (1976*a*) the clump magnitude is obvious, but the giant branch is poorly populated. Most red-giant branches lie a few hundredths of a magnitude to the red of the clump in open clusters. If the apparent location of the giant branch in NGC 2204 as seen in Figure 3 of Hawarden (1976*a*) and Figure 1 of Dawson (1981) is correct, the separation is almost 0.15 mag in this cluster. Assuming that these red stars are nonmembers or are unrepresentative of the true giant branch location, a typically bluer red-giant branch would indicate an age based on cluster morphology closer to NGC 2506's than NGC 752's. More accurate giant-branch photometry and membership information on these stars would be helpful as a test of the apparent anomaly.

NGC 2420.—Reddening and metallicity: McClure, Forrester, and Gibson (1974); age: McClure, Twarog, and Forrester (1981); cm diagram: McClure, Newell, and Barnes (1978).

NGC 2506.—Reddening, metallicity, age, cm diagram: McClure, Twarog, and Forrester (1981).

M67.—Reddening: Taylor (1978), Janes and Smith (1984); metallicity: Eggen and Sandage (1964), Janes and Smith (1984): age: Twarog (1978); cm diagram: Eggen and Sandage (1964), Racine (1971).

The value of 3.5×10^9 yr for the cluster age derived by TW has been increased to 4.0×10^9 yr to compensate for the lower metallicity implied by recent photometric estimates of the cluster abundance (Janes and Smith 1984, Eggen 1983).

Melotte 66.—Reddening and metallicity: Hawarden (1976*b*), Dawson (1978); age: Anthony-Twarog, Twarog, and McClure (1979); cm diagram: Hawarden (1976*b*), Anthony-Twarog, Twarog, and McClure (1979).

Though this cluster is unusually important because it ties down the high end of the age scale, it is also an unusually weak data point because the cluster is now known to suffer variable reddening to a serious degree (Hawarden 1980, private communication). From Figure 2 of Anthony-Twarog, Twarog, and McClure (1979) this has only a minor effect on the definition of the giant-branch parameters, but makes age determination by comparison of the turnoff to isochrones and the derivation of the turnoff parameters for the MAR very uncertain. The mean color of the turnoff has been adopted for use in the MAR and for age estimation from isochrone fits. The magnitude of the turnoff has been obtained by ignoring the stars above the apparent gap at $V = 16.7$. It is felt that these stars represent a population similar to that found above the turnoffs of NGC 2420 and NGC 2506; the gap and stellar sequence are better defined simply because of the rich nature of the cluster. Thus, the MAR should be regarded as a probable upper limit for the cluster.

REFERENCES

Anthony-Twarog, B. J., and Demarque, P. 1977, *Astr. Ap.,* **57,** 471.
Anthony-Twarog, B. J., Twarog, B. A., and McClure, R. D. 1979, *Ap. J.,* **233,** 188.
Blanco, V. M. 1982, *Pub. A.S.P.,* **94,** 201.
Burstein, D., and Heiles, C. 1982, *A.J.,* **87,** 1165.
Cannon, R. D. 1970, *M.N.R.A.S.,* **150,** 111.
Christian, C. A., and Janes, K. A. 1979, *A.J.,* **84,** 204.

Ciardullo, R. D., and Demarque, P. 1977, *Trans. Yale Univ. Obs.,* **33,** 1.
———. 1979, in *Dudley Obs. Report 14, Problems of Calibration of Multicolor Photometric Systems,* ed. A. G. D. Philip, p. 317.
Crawford, D. L., and Mandwewala, N., 1977, *Publ. A.S.P.,* **88,** 917.
Da Costa, G. S., Mould, J., and Ortolani, S. 1984, *Ap. J.,* **282,** 125.
Dawson, D. W. 1978, *A.J.,* **83,** 1424.
———. 1981, *A.J.,* **86,** 237.

Demarque, P., and McClure, R. D. 1977, in *Evolution of Galaxies and Stellar Populations*, ed. B. M. Tinsley and R. B. Larson (New Haven: Yale Univ. Obs.), p. 199.

Eggen, O. J. 1963, *Ap. J.*, **138**, 356.

———. 1983, *A.J.*, **88**, 813.

Eggen, O. J., and Sandage, A. 1964, *Ap. J.*, **140**, 130.

———. 1969, *Ap. J.*, **158**, 669.

FitzGerald, M. P. 1970, *Astr. Ap.*, **4**, 234.

Frogel, J. A., and Twarog, B. A. 1983, *Ap. J.*, **274**, 270.

Hanson, R. B. 1975, *A.J.*, **80**, 379.

Harris, W. E. 1976, *A.J.*, **81**, 1095.

Harris, W. E., and Canterna, R. 1981, *A.J.*, **86**, 1332.

Hartwick, F. D. A. 1968, *Ap. J.*, **154**, 475.

Hawarden, T. G. 1971, *Observatory*, **91**, 78.

———. 1976a, *M.N.R.A.S.*, **174**, 225.

———. 1976b, *M.N.R.A.S.*, **174**, 471.

Iben, I. 1974, *Ann. Rev. Astr. Ap.*, **12**, 215.

Janes, K. A. 1984, preprint.

Janes, K. A., and Smith, G. H. 1984, *A.J.*, **89**, 487.

Johnson, H. L. 1953, *Ap. J.*, **117**, 356.

Kinman, T. D. 1965, *Ap. J.*, **142**, 655 (KI).

Kunth, D., and Sargent, W. L. W. 1983, *Ap. J.*, **273**, 81.

Lequeux, L. 1979, *Astr. Ap.*, **80**, 35.

Liller, M. H. 1980, *A.J.*, **85**, 1480 (LI).

McClure, R. D. 1974, *Ap. J.*, **194**, 355.

McClure, R. D., Forrester, W. T., and Gibson, J. 1974, *Ap. J.*, **189**, 409.

McClure, R. D., Newell, B., and Barnes, J. V. 1978, *Pub. A.S.P.*, **90**, 170.

McClure, R. D., and Twarog, B. A. 1977, *Ap. J.*, **214**, 111.

McClure, R. D., Twarog, B. A. and Forrester, W. T. 1981, *Ap. J.*, **243**, 841.

Peimbert, M., and Serrano, A. 1980, *Rev. Mexicana Astr. Ap.*, **5**, 9.

Perrin, M.-N., Hejlesen, P. M., Cayrel de Strobel, G., and Cayrel, R. 1977, *Astr. Ap.*, **54**, 779.

Pilachowski, C. A. 1984, preprint.

Racine, R. 1971, *Ap. J.*, **168**, 393.

Sandage, A. 1969, *Ap. J.*, **157**, 515.

———. 1982, *Ap. J.*, **252**, 553.

Sandage, A., and Wallerstein, G. 1960, *Ap. J.*, **131**, 598.

Spinrad, H., and Taylor, B. J. 1971, *Ap. J.*, **163**, 303.

Talent, D. 1980, Ph.D. thesis, Rice University.

Taylor, B. J. 1978, *Ap. J. Suppl.*, **36**, 173.

Twarog, B. A. 1978, *Ap. J.*, **220**, 890 (TW).

———. 1983a, *Bull. AAS*, **15**, 645.

———. 1983b, *Ap. J.*, **267**, 207.

VandenBerg, D. A. 1983, *Ap. J. Suppl.*, **51**, 29 (VB).

VandenBerg, D. A., and Bridges, T. J. 1984, *Ap. J.*, **278**, 679.

BARBARA J. ANTHONY-TWAROG and BRUCE A. TWAROG: Department of Physics and Astronomy, University of Kansas, Lawrence, KS   66045